

Categorical Groups, Knots and Knotted Surfaces

João Faria Martins*

March 5, 2019

Abstract

We define a knot invariant and a 2-knot invariant from any finite categorical group.

Introduction

In [Y], David Yetter defines an invariant of piecewise linear manifolds from any finite categorical group, or, what is the same, from any finite crossed module $\mathcal{G} = (G, E, \partial, \triangleright)$, see [BM] or [BS]. The meaning of Yetter's construction was elucidated further by Tim Porter in [P].

The invariant discovered by Yetter is defined from triangulations of manifolds equipped a strict order relation on its set of vertices. Loosely speaking, it counts, apart from normalising factors, the number of ways we can colour the edges of the triangulation by elements of G and of its faces by elements of E in a coherent way as displayed in figure 1, and so that for each tetrahedron the faces of each ordered simplex commute as a diagram in $C(\mathcal{G})$, the tensor category constructed from \mathcal{G} , in other words the categorical group associated with \mathcal{G} (we will explain this construction below). This last constraint can be seen as a flatness condition. The aim of this article to present a method for calculating this invariant for the case in which the manifold is a knot complement or the 4 dimensional complement of a knotted surface, therefore defining a class of knot and 2-knot invariants. These invariants depend only

*email address: jmartins@math.ist.utl.pt

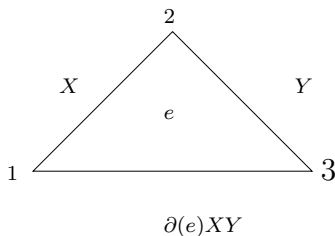


Figure 1: Coherent colouring of a simplex

on the homotopy 2-type of the complements, similarly to Yetter’s invariants of manifolds.

With a bit of work, any manifold invariant defined from triangulations can be described in such way that it can be calculated from handle decompositions of manifolds, which are more flexible than triangulations¹. For the case of Yetter’s invariant, one would consider colourings of 1-handles by elements of G and of 2-handles by elements of E , coherent in a similar sense as above. The handles of index 3 must, like tetrahedrons, be assigned flatness conditions.

Given a knot diagram or a movie representation of a knotted surface, there are very natural handle decompositions of the complement of a regular neighbourhood of any of them. We will not give a precise description of Yetter’s invariant in terms of handle decompositions of manifolds. Rather, we will associate a state sum to every knot diagram and any movie of a knotted surface, which is inspired by natural handle decompositions of the complements as well as Yetter’s construction, and prove directly that they are topological invariants.

This article is independent of Yetter’s results, although it retains most of his construction’s philosophy. Nevertheless, it does introduce new techniques and results.

It is hoped these descriptions will shed some light on how to define invariants of 2-knots from crossed modules of quantum groups. Another possible direction could be trying to define what a categorical quandle is.

¹This is a lesson I learnt from Dr John W. Barrett

1 The Categorical Setting

1.1 Crossed Modules and Categorical Groups

Let G and E be groups. A crossed module with base G and fibre E , say $\mathcal{G} = (G, E, \partial, \triangleright)$, is given by a group morphism $\partial : E \rightarrow G$ and an action \triangleright of G on E on the left by automorphisms. The conditions on \triangleright and ∂ are:

1. $\partial(X \triangleright e) = X \partial(e) X^{-1}; \forall X \in G, \forall e \in E$.
2. $\partial(e) \triangleright f = e f e^{-1}; \forall e, f \in E$.

Let \mathcal{G} be a crossed module. We can define a strict tensor category $\mathcal{C}(\mathcal{G})$ from it. The set of objects of $\mathcal{C}(\mathcal{G})$ is given by all elements of G . Given a $X \in G$, the set of all morphisms with source X is E , and the target of $e \in E$ is $\partial(e)X$. In other words a morphism in $\mathcal{C}(\mathcal{G})$ “looks like” $X \xrightarrow{e} \partial(e)X$. Given $X \in G$ and $e, f \in E$ the composition

$$X \xrightarrow{e} \partial(e)X \xrightarrow{f} \partial(f)\partial(e)X$$

is

$$X \xrightarrow{fe} \partial(fe)X.$$

The tensor product has the form

$$\begin{array}{ccc} X & Y & XY \\ \downarrow e & \otimes & \downarrow f \\ \partial(e)X & \partial(f)Y & \partial(e)X\partial(f)Y \end{array} = \begin{array}{c} XY \\ \downarrow eX \triangleright f \end{array} . \quad (1)$$

From the definition of a crossed module, it is easy to see that we have indeed defined a strict tensor category. This construction is an old one. The tensor category $\mathcal{C}(\mathcal{G})$ is a categorical group (see [BM] and [BS]). It is well known that the categories of crossed modules and of categorical groups are equivalent (see [BS]). We skip further details on this connection since the point we want to emphasise is that we can construct a category $\mathcal{C}(\mathcal{G})$ from any crossed module.

1.2 Duality

The category $\mathcal{C}(\mathcal{G})$ admits a strict pivotal structure, see [BW1], [BW2] or [FY], for which the duality contravariant functor is

$$\left(X \xrightarrow{e} \partial(e)X \right)^* = \left(X^{-1} \partial(e^{-1}) \xrightarrow{X^{-1} \triangleright e} X^{-1} \right). \quad (2)$$

From the definition of a crossed module, it is immediate that $*$ is a contravariant functor. Given an object X of $\mathcal{C}(\mathcal{G})$, there exists an arrow $\varepsilon_X = \left(1_G \xrightarrow{1_E} X \otimes X^*\right)$. With these arrows and the duality contravariant functor $*$, the category $\mathcal{C}(\mathcal{G})$ is a strict pivotal category, in other words verifies the conditions of definitions 2.1 and 2.2 of [BW2]. Equation 1 is used frequently to prove this. Warning: in general this category is not spherical.

2 A State Sum Invariant of knots

We now define an invariant of knots, or strictly speaking of dotted oriented links in which each component has at least one bivalent vertex. A dotted link is a link possibly with some extra bivalent vertices inserted.

2.1 Motivation and Construction

Let $D_L \subset \mathbb{R}^2$ be a dotted link diagram of the dotted link L . We thus have a handle decomposition of the complement of L for which each arc of the projection generates a 1-handle, and each vertex or crossing generates a 2-handle. We have a unique 0-handle around the "eye of the observer" and a unique 3-handle opposite him/her. Notice that since each link we consider is supposed to have at least a bivalent vertex, there is not the danger that an arc of the projection may be a loop. This construction is similar to the one in [BGM], 3.2. Such type of handle decompositions of knot complements motivates the definition of flat colourings of knot diagrams.

2.1.1 Colourings of Knot Diagrams

Let $\mathcal{G} = (G, E, \partial, \triangleright)$ be a crossed module. Suppose D_L is an oriented dotted link diagram of the oriented dotted link L . It determines a 4/2-valent oriented graph $\Gamma(D_L)$ embedded in \mathbb{R}^2 .

Definition 1 *A \mathcal{G} -colouring c of D_L is a colouring c of the edges and the vertices of the graph $\Gamma(D_L)$ by objects and morphisms of $\mathcal{C}(\mathcal{G})$, respectively, coherent with the categorical structure of $\mathcal{C}(\mathcal{G})$, which in the areas determined by the vertices and crossings looks like figure 2.*

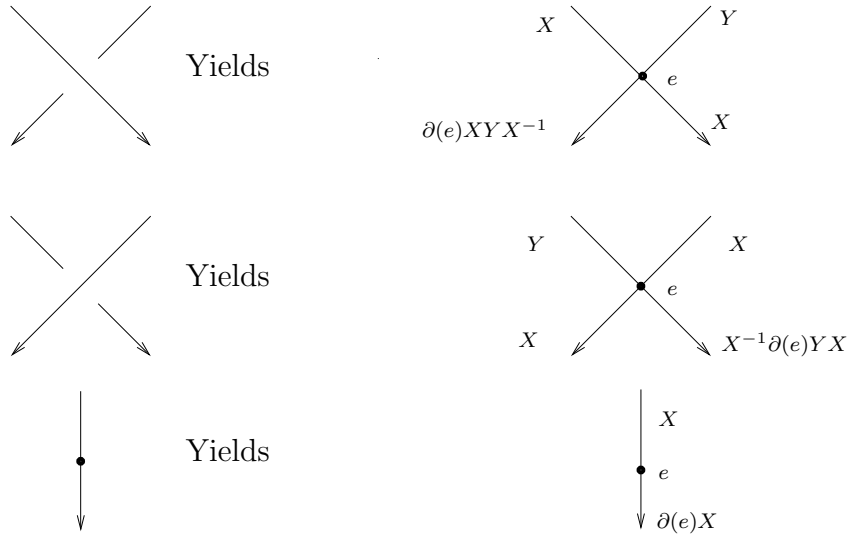


Figure 2: A bit of a \mathcal{G} -colouring of a dotted link diagram

2.1.2 Flat Colourings and the State Sum

Let L be a dotted link and D_L one of its diagrams. Let also $\mathcal{G} = (G, E, \partial, \triangleright)$ be a crossed module which we suppose finite. A \mathcal{G} -colouring c of D_L , determines a coloured graph $\Gamma(D_L, c)$ embedded in \mathbb{R}^2 , such that the edges of $\Gamma(D_L)$ are coloured with objects of $\mathcal{C}(\mathcal{G})$, and such that at each vertex of $\Gamma(D_L)$ we have a morphism from the tensor product of the objects assigned to the incoming edges of it to the tensor product of the objects associated to the outgoing edges of it. Recall that the category $\mathcal{C}(\mathcal{G})$ is a strict pivotal category. Therefore, by a theorem of coherence due to John W. Barrett and Bruce Westbury, see [BW1], this coloured graph $\Gamma(D_L, c)$ can be evaluated to give a morphism $1_G \xrightarrow{\langle \Gamma(D_L, c) \rangle} 1_G$. This morphism only depends on the planar (but in general not S^2) isotopy class of $\Gamma(D_L, c)$. See also [FY].

Definition 2 A colouring c of a dotted link diagram D_L is said to be flat if:

$$\langle \Gamma(D_L, c) \rangle = 1_E. \quad (3)$$

Let D_L be a dotted link diagram of L . Define

$$I(D_L) = \frac{\#\{\text{flat colourings of } D_L\}}{\#E\#\{\text{vertices of } \Gamma(D_L)\}}. \quad (4)$$

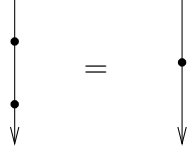


Figure 3: Simplest vertex move

Exercise 1 *Let O be the unknot with a vertex inserted. Prove that*

$$I(O) = \frac{\#G}{\#E}.$$

Remark 3 *Flatness is not necessary, but ensures non triviality.*

2.2 Invariance

We now sketch the proof that $I(D_L)$ is a topological invariant.

2.2.1 Invariance Under Moves of an Isolated Vertex

First of all the following holds:

Lemma 4 *The state sum $I(D_L)$ is invariant under the move of figure 3.*

The method of proof of the invariance under this move generalises to the other ones, the reason why we will present it in full detail. Given a dotted link diagram D , let $C(D)$ be the set of flat colourings of D .

Proof. Let the diagrams D and D' differ by the move in figure 3. Consider the map $F : C(D) \rightarrow C(D')$ defined in figure 4, with no changes outside the rectangle. It is obvious that it sends flat colourings to flat colourings since the morphisms of $\mathcal{C}(\mathcal{G})$ inside the rectangle in D and D' are the same, namely $X \xrightarrow{fe} \partial(fe)X$. Obviously the map F is surjective and its fibre at each point (in other words the inverse image at each point) has the same cardinality as E , which finishes the proof. ■

Secondly:

Lemma 5 *The state sum $I(D)$ is invariant under the moves of figure 5.*

Proof. Let us prove the upper left corner. The proof for the other cases is analogous. Let D and D' be link diagrams differing by the upper left move

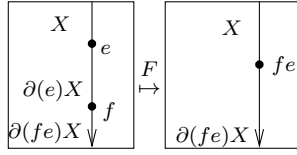


Figure 4: A map between colourings

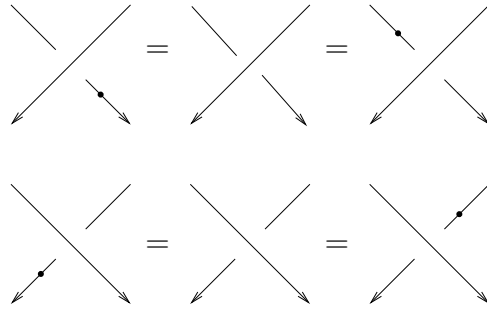


Figure 5: Second simplest vertex moves

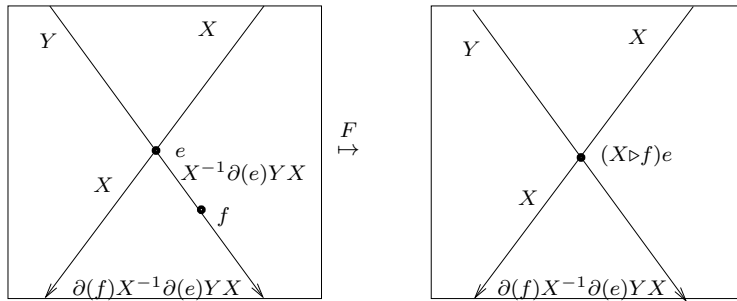


Figure 6: A map between colourings



Figure 7: Remaining vertex moves

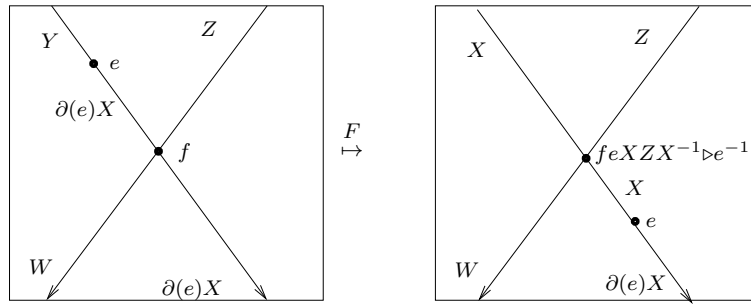


Figure 8: A map between colourings. Here $W = \partial(f)\partial(e)XZX^{-1}\partial(e^{-1}) = \partial(f)\partial(e)\partial(XZX^{-1}\triangleright e^{-1})XZX^{-1}$

in figure 5. We define a map $F : C(D) \rightarrow C(D')$ as in figure 6, where the rest of the colouring remains unaltered.

As before, F transforms flat colourings into flat colourings. This is because in both cases the morphism in $\mathcal{C}(\mathcal{G})$ inside the square is the same because of equation (1). This morphism is $YX \xrightarrow{(X\triangleright f)e} \partial(X\triangleright f)\partial(e)XY = X\partial(f)X^{-1}\partial(e)YX$. Obviously F is surjective and the fibre at each point has the same cardinality as E . ■

Next we have:

Lemma 6 *The state sum $I(D)$ is invariant under the moves of figure 7.*

Proof. We prove bit on the left. Let D and D' differ by this move. We define a map $F : C(D) \rightarrow C(D')$ as in figure 8. To prove it transforms flat colourings into flat colourings notice that $(W\triangleright e)feXZX^{-1}\triangleright e^{-1} = fe$ (c.f. equation (1)). Obviously F is a bijection. ■

2.2.2 Invariance Under Reidemeister-I

Since we are considering oriented knot diagrams, there are four different cases of the Reidemeister-I move, considered up to planar isotopy. They are

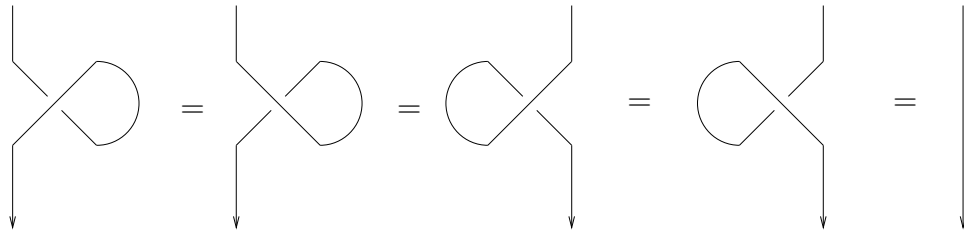


Figure 9: Different Cases of Reidemeister-I

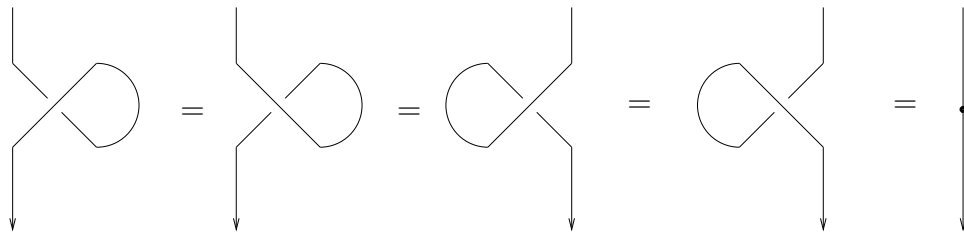


Figure 10: Identity used to prove invariance under Reidemeister-I

depicted in figure 9.

This Reidemeister move is the easiest to verify. This is because of the identities of figure 9. Therefore, we can apply the results of 2.2.1. In particular they tell us that vertices can be absorbed by the rest of the diagram. We omit the details since more intricate calculations will follow.

2.2.3 Invariance Under Reidemeister-II

There are four different kinds of oriented Reidemeister-II moves. They are obtained from figure 11 through considering all the possible orientations of the two strands.

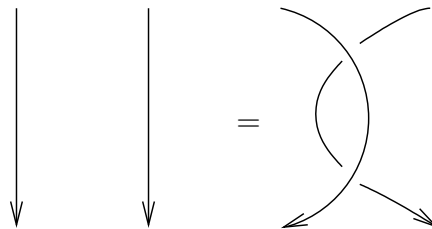


Figure 11: One variant of the Reidemeister-II move

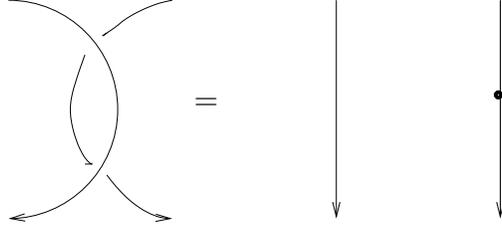


Figure 12: Identity used to prove invariance under Reidemeister-II move

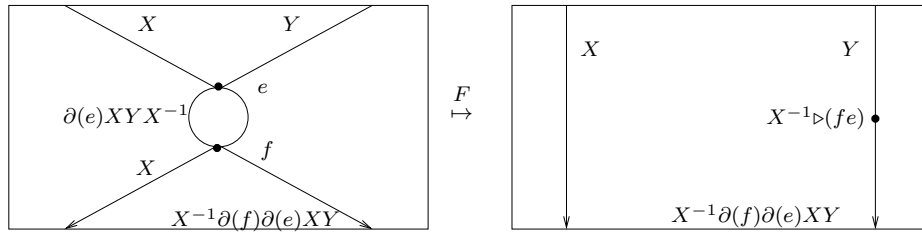


Figure 13: Map used to prove invariance under Reidemeister-II

Let D be D' be knot diagrams differing by a Reidemeister move of type II. We can suppose by 2.2.1 that both diagrams have at least one vertex. Therefore, all is obvious from the identity in figure 12 (and its counterparts for other orientations of the strands), together with 2.2.1. To prove it use the map $F : C(D) \rightarrow C(D')$ of figure 13. Notice it sends flat colourings to flat colourings since in both cases the morphism inside the rectangle is $XY \xrightarrow{fe} \partial(fe)XY$. As before F is surjective and its fibre has the same cardinality as E .

2.2.4 Invariance Under Reidemeister-III

This is the most difficult move. Since we are considering oriented knot diagrams, there are sixteen versions of the Reidemeister move number III. They are obtained from the move in figure 14, through considering the mirror image as well as all possible orientations of the strands.

Let D and D' differ by a Reidemeister-III. Suppose it is of the kind depicted in figure 14. We leave as an exercise to prove that the equalities $a = e$, $b = (Y^{-1} \triangleright e^{-1})(Y^{-1}Z \triangleright g)$ and $c = f(X \triangleright e)$ in figure 15, define a one-to-one map between colourings of D and colourings of D' . Notice that we always have $a(Y \triangleright b)c = (Z \triangleright g)f(X \triangleright e)$ (recall equation (1)), which

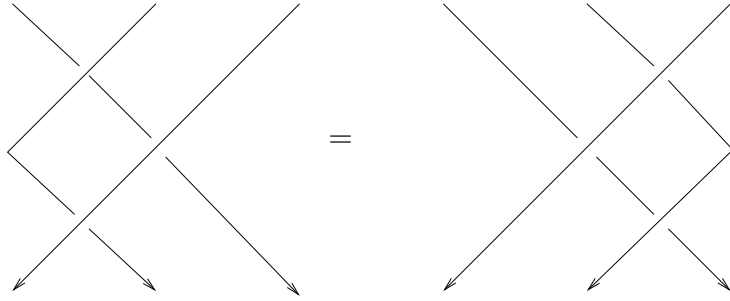


Figure 14: Reidemeister-III

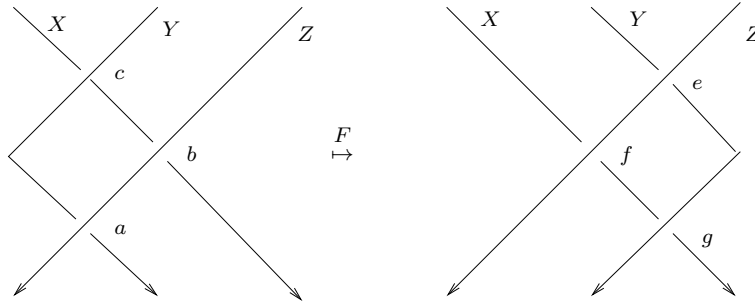


Figure 15: Map used to prove invariance under Reidemeister-III move, first case

implies that flat colourings are always sent to flat colourings under the map just defined. The proof of invariance for the other types of Reidemeister-III is analogous. For example for the mirror image of figure 14, we use the map of figure 16 to prove invariance. Here $g = ca$, $f = YX^{-1} \triangleright bYZY^{-1}X^{-1} \triangleright a^{-1}$ and $e = a$. This map transforms flat colourings into flat colourings since $c(\partial(a)XYX^{-1} \triangleright b)a = caXYX^{-1} \triangleright b = (W \triangleright e)g(X \triangleright f)$.

2.2.5 Planar Deformations

The invariance of $I(D)$ under horizontal deformations is an obvious consequence of the general theorem of coherence for pivotal categories, see [BW1] or [FY]. As mentioned in 2.1.2, evaluations of colourings are invariant under planar deformations, thus flat colourings are sent to flat colourings under planar deformations. This finishes the proof that $I(D)$ is a topological invariant. We thus have a knot invariant for any finite crossed module.

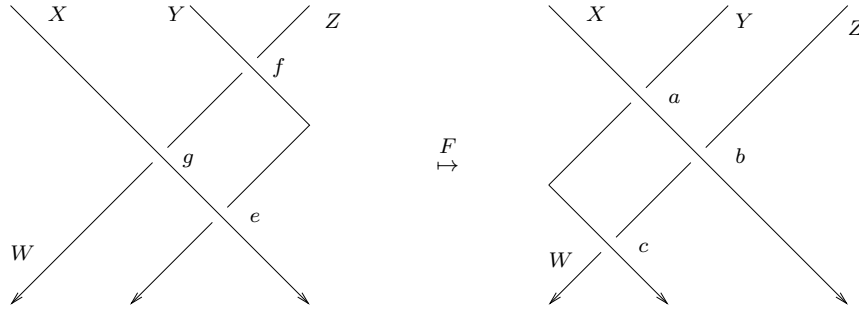


Figure 16: Map used to prove invariance under Reidemeister-III move, second case. Here $W = \partial(c)\partial(a)XYX^{-1}\partial(b)XZY^{-1}X^{-1}\partial(a^{-1})$

Remark 7 *Despite the fact that we need to consider oriented knot diagrams to define our invariant, it is easy to verify that our invariant does not depend on the orientations chosen.*

3 Knotted Surfaces

As usual, we fix a finite crossed module $\mathcal{G} = (G, E, \partial, \triangleright)$.

For details on knotted surfaces see [CS]. Consider an embedded surface Σ in $S^4 = R^4 \cup \{\infty\}$, or in general an embedding in codimension 2. Suppose the projection in the last variable is a Morse function in Σ , thus determining a handle decomposition of Σ . Let $\nu(\Sigma)$ be a regular neighbourhood of Σ in S^4 . We then have a natural handle decomposition of $S^4 \setminus \nu(\Sigma)$, where a regular neighbourhood of each a -handle of Σ intersects complementary a unique $a + 1$ handle of $S^4 \setminus \nu(\Sigma)$, see [GS], 6.2. This is very easy to visualise in dimension 3. Therefore, considering the movie of the chosen embedding of Σ , births of circles will induce 1-handles in the handle decomposition of the complement, and therefore must be assigned elements of G ; saddle points induce 2-handles of the complement, thus must be coloured by elements of E , coherently; and deaths of circles correspond to 3-handles in the complement, thus must correspond to flatness conditions.

However, in general when considering the Kirby Diagram of this handle decomposition, the attaching regions of 2-handles are only determined up to handle slides, which causes an extra complication in our combinatorial framework. This problem is solved below by considering a set of relations on dotted knot diagrams.

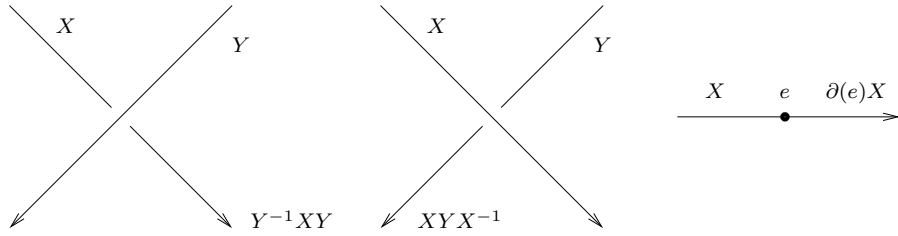


Figure 17: Definition of a colouring of a dotted knot diagram

3.1 A Vector Space Associated with Knot Diagrams

Let us fix a ground field κ . Recall that a dotted knot diagram is by definition a regular projection of a bivalent graph, in other words of a link possibly with some extra bivalent vertices inserted. Let D be a dotted knot diagram as before oriented. Let also $\mathcal{G} = (G, E, \triangleright, \partial)$ be a finite crossed module.

Definition 8 *A colouring of D is an assignment of elements of G to the arcs of D and elements of E to the vertices of D verifying the conditions of figure 17.*

Warning 9 *The definition of a colouring of a dotted knot diagram is different of the one given previously in the 3-dimensional case.*

Remark 10 *As in the 3-dimensional case, a \mathcal{G} -colouring of a dotted knot diagram D determines a colouring of the vertices and the edges of the 4/2-valent graph determined by D , by objects and morphisms of $\mathcal{C}(G)$, the tensor category made from \mathcal{G} . However, in this case, the 4-valent vertices are always assigned the trivial morphism. Nevertheless, the important observation is that, as in 2.1.2, colourings of dotted knot diagrams can always be evaluated to give morphisms in $\mathcal{C}(\mathcal{G})$.*

Definition 11 *Let D be a knot diagram. A dotting of D is an insertion of bivalent vertices on D considered up to planar isotopy. If D is a knot diagram, let $V(D)$ be the free vector space on the set of all colourings of all dottings of D .*

Consider now the relations of figures 18, 19 and 20. It is straightforward to see that they are local on the knot diagrams and that they transform colourings into colourings.

$$\begin{array}{ccc}
\begin{array}{c} X \quad \quad \quad 1_E \quad \quad \quad X \\ \hline \bullet \\ \hline \longrightarrow \end{array} & = & \begin{array}{c} X \\ \hline \longrightarrow \end{array} \quad R1 \\
\begin{array}{c} X \quad e \quad \partial(e)X \quad f \quad \partial(fe)X \\ \hline \bullet \quad \quad \quad \bullet \\ \hline \longrightarrow \end{array} & = & \begin{array}{c} X \quad \quad \quad fe \quad \quad \quad \partial(fe)X \\ \hline \bullet \\ \hline \longrightarrow \end{array} \quad R2
\end{array}$$

Figure 18: Relations on colourings

Remark 12 Notice that in all cases the morphisms in $\mathcal{C}(\mathcal{G})$ evaluated considering the colouring of both sides of the relations R1 to R6 (c.f. remark 10) are always the same.

Definition 13 Let D be an oriented knot diagram (without vertices). The vector space $\mathcal{V}(D)$ is defined as the vector space obtained from $V(D)$ by considering the relations R1 to R6.

3.2 Reidemeister Moves

We now prove that if D and D' are related by Reidemeister moves, then there are naturally associated linear maps $\mathcal{V}(D) \rightarrow \mathcal{V}(D')$. If m is such a move, call this linear map $F(m)$.

3.2.1 Reidemeister-I

As pointed out in the second chapter, since we are considering oriented knot diagrams, there are four different cases of the Reidemeister-I move, considered up to planar isotopy. Suppose D' is related to D by a positive Reidemeister-I move m , positive means it transforms a straight strand into a kink. Define a map $\mathcal{V}(D) \xrightarrow{F(m)} \mathcal{V}(D')$ as in figure 21. Only one kind of Reidemeister-I is shown, but the other cases are perfectly analogous. To prove $F(m)$ is well defined, we need to prove the equality of figure 22. This is done in figure 23. The proof for the other cases is analogous. It is trivial to conclude that $F(m)$ is a vector space isomorphism, therefore its inverse exists. This will define $F(m^{-1}) = F(m)^{-1}$ for the negative Reidemeister-I move.

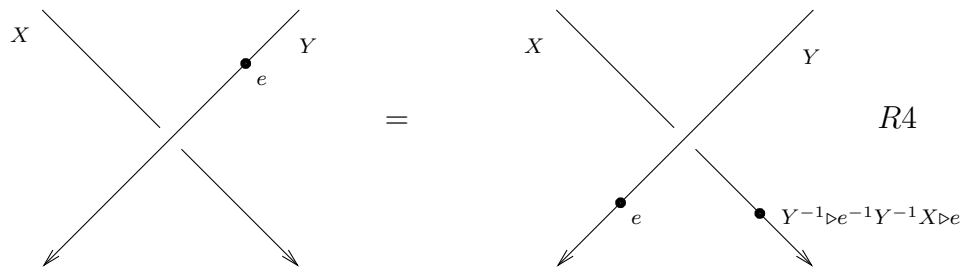
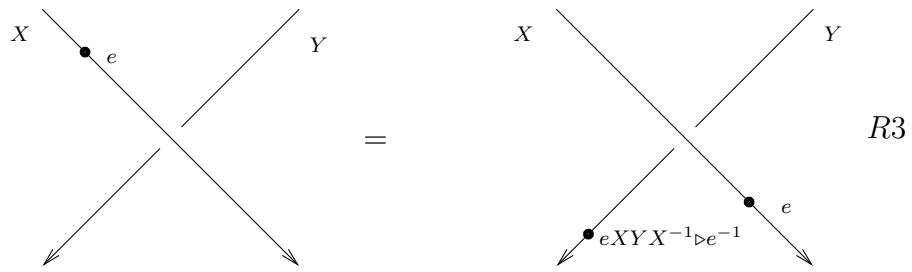


Figure 19: Relations on colourings

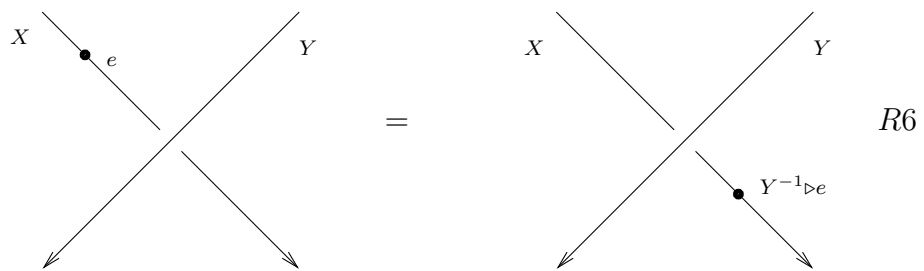
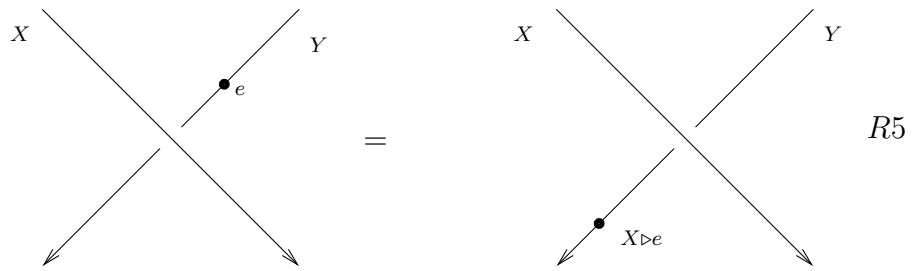


Figure 20: Relations on colourings

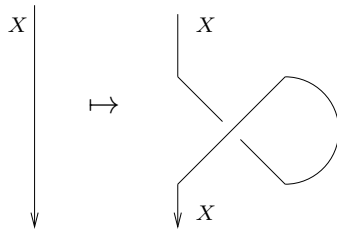


Figure 21: Map associated to positive Reidemeister-I move

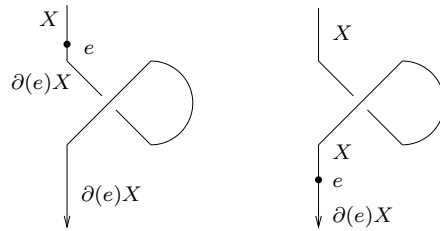


Figure 22: Identity needing proof

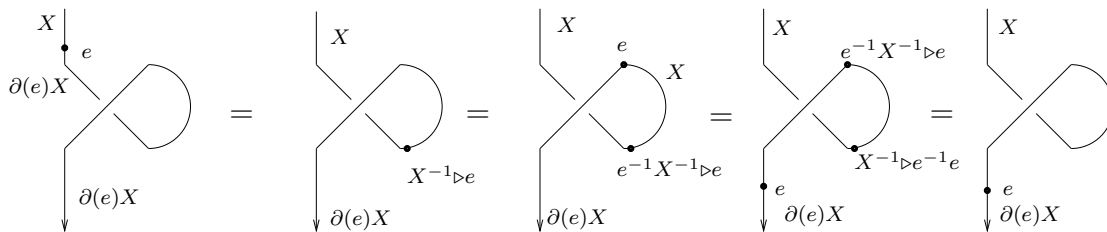


Figure 23: Proof of the identity in figure 22

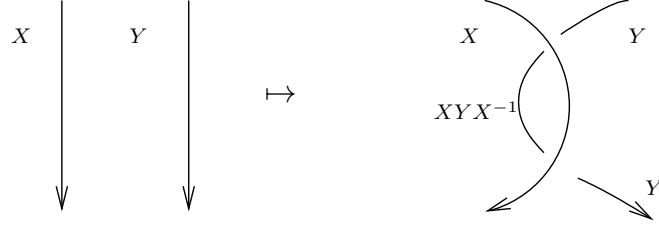


Figure 24: Map assigned to Reidemeister-II

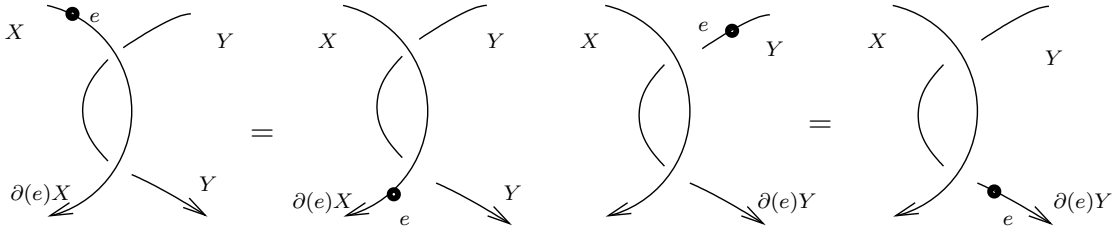


Figure 25: Two identities that need proving

3.2.2 Reidemeister-II

Let D and D' be knot diagrams differing by Reidemeister move number II. Call it m . Define a map $\mathcal{V}(D) \xrightarrow{F(m)} \mathcal{V}(D')$ as in figure 24. The definition of $F(m)$ for the other types of Reidemeister-II moves is analogous. To prove that $F(m)$ is well defined, we need to prove the equalities of figure 25. The most difficult one is the first and the proof of it appears in figure 26. The last identity follows from

$$\begin{aligned}
& X^{-1} \triangleright e^{-1} X^{-1} \partial(e) X Y X^{-1} \partial(e^{-1}) \triangleright e X^{-1} \triangleright (e X Y X^{-1} \triangleright e^{-1}) \\
&= X^{-1} \triangleright e^{-1} X^{-1} \triangleright e Y X^{-1} \triangleright e X^{-1} \triangleright e^{-1} X^{-1} \triangleright e Y X^{-1} \triangleright e^{-1} \\
&= X^{-1} \triangleright e^{-1} X^{-1} \triangleright e Y X^{-1} \triangleright e Y X^{-1} \triangleright e^{-1} \\
&= 1_E
\end{aligned}$$

Notice that if m is a positive Reidemeister-II move between the diagrams D and D' then the map $\mathcal{V}(D) \xrightarrow{F(m)} \mathcal{V}(D')$ is a vector space isomorphism, which defines $F(m)^{-1} : \mathcal{V}(D') \rightarrow \mathcal{V}(D)$.

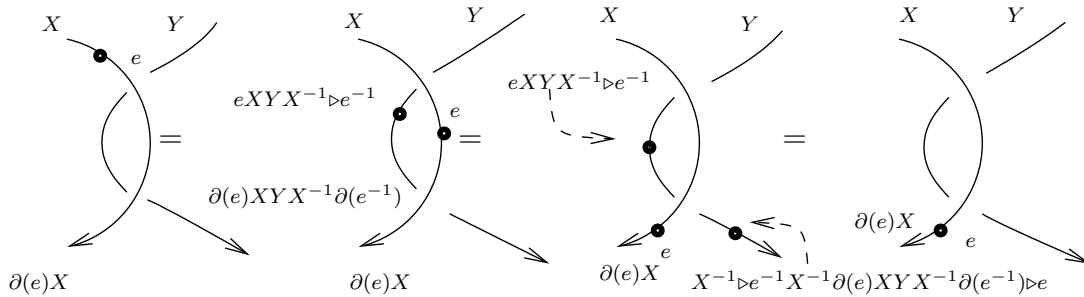


Figure 26: Proof of identity 25

3.2.3 Some Commutation Relations

The relations $R1$ to $R6$ commute with each others in the sense presented in figures 27, 28, 29. They have obvious counterparts for diagrams with different crossing information.

3.2.4 Reidemeister-III

As we mentioned in the second chapter, since we are considering oriented knot diagrams, there are sixteen versions of the Reidemeister move number III. The positive move has the direction indicated in the figure 14. Let D and D' differ by a Reidemeister-III move m . Suppose we have a dotting of D . We can always move the vertices away from the area in question. For definiteness, suppose we move all vertices in the direction defined by the orientation of the edges, starting with the top strand and finishing with the bottom one. This operation verifies the relations $R1$ to $R6$ due to the commutation relation presented in 3.2.3. Having done these changes, the definition of $\mathcal{V}(D) \xrightarrow{F(m)} \mathcal{V}(D')$ is straightforward and appears in figure 30. It is analogous for the other types of Reidemeister-III moves. To prove $F(m)$ is well defined we still need to prove a set of relations similar to the relations in figures 22 and 25, and then apply the results of 3.2.3. The proof of the

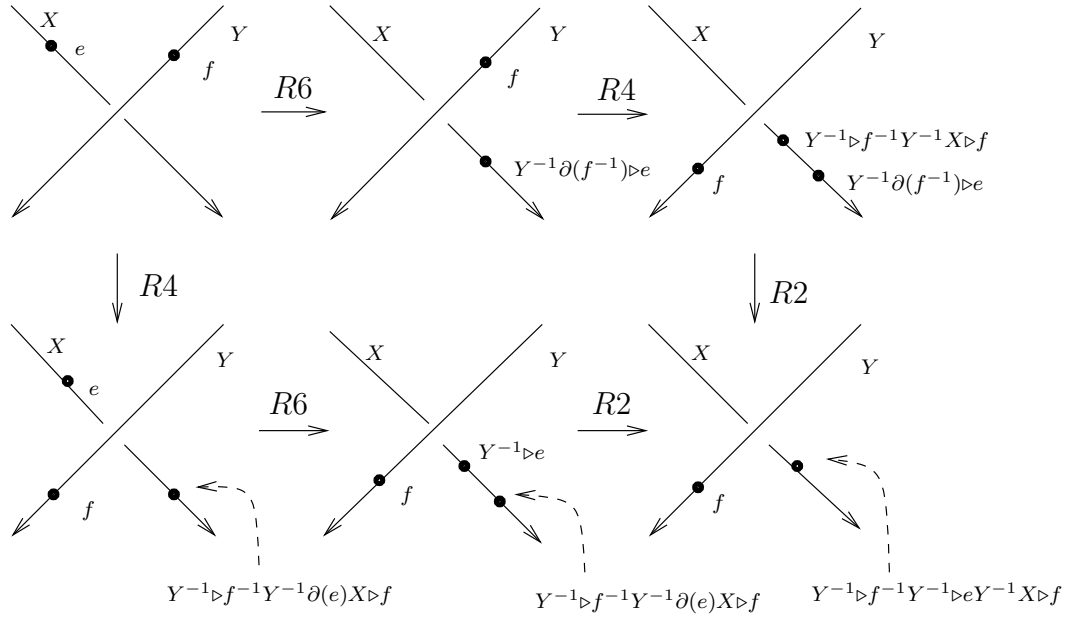


Figure 27: A commutation relation

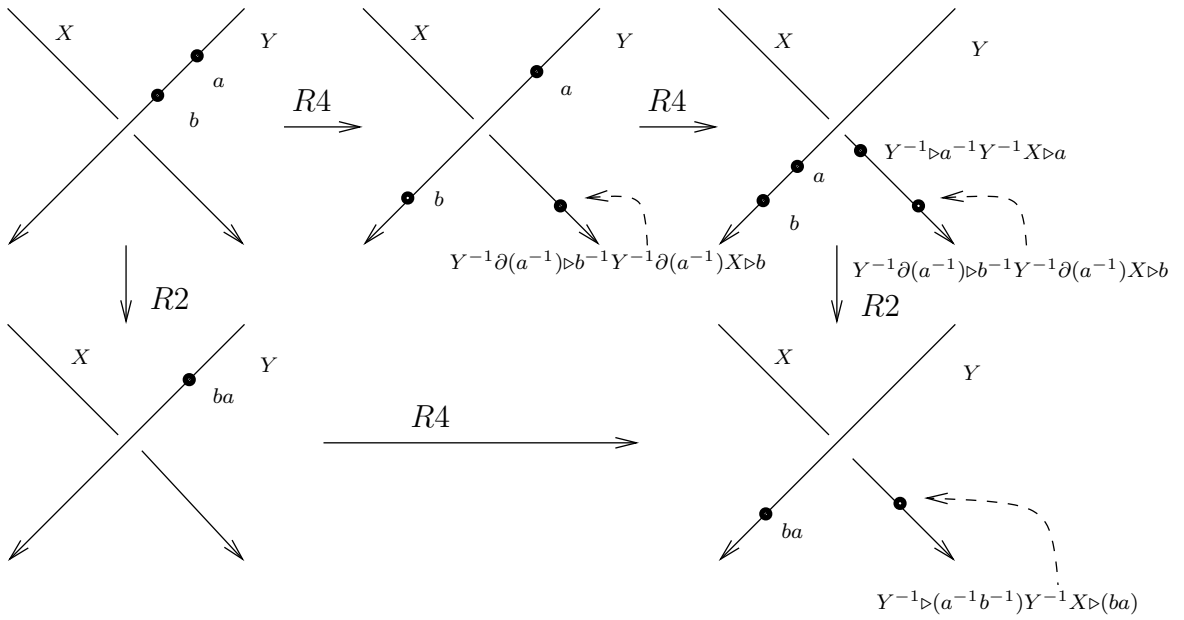


Figure 28: A commutation relation

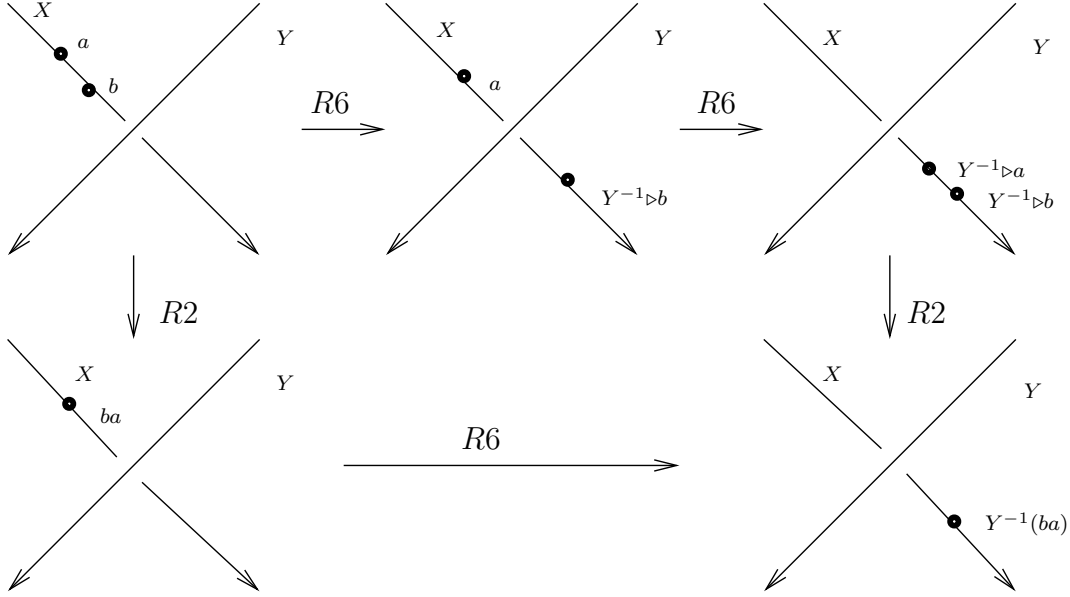


Figure 29: A commutation relation

most difficult one appears in figure 31. The last equality follows from:

$$\begin{aligned}
& (Z^{-1} \triangleright e^{-1} Z^{-1} Y^{-1} \triangleright e Z^{-1} Y^{-1} \partial(e^{-1}) X \partial(e) \triangleright e^{-1} Z^{-1} Y^{-1} \partial(e^{-1}) X \partial(e) Y \triangleright e) \\
& \quad Z^{-1} Y^{-1} Z \triangleright (Z^{-1} \triangleright e^{-1} Z^{-1} X \triangleright e) \\
& = Z^{-1} \triangleright e^{-1} Z^{-1} Y^{-1} \triangleright e Z^{-1} Y^{-1} \triangleright e^{-1} Z^{-1} Y^{-1} X \triangleright e^{-1} Z^{-1} Y^{-1} \triangleright e \\
& \quad Z^{-1} Y^{-1} \triangleright e^{-1} Z^{-1} Y^{-1} X \triangleright e Z^{-1} Y^{-1} X Y \triangleright e Z^{-1} Y^{-1} X \triangleright e^{-1} Z^{-1} Y^{-1} \triangleright e \\
& \quad \quad Z^{-1} Y^{-1} \triangleright e^{-1} Z^{-1} Y^{-1} X \triangleright e \\
& = Z^{-1} \triangleright e^{-1} Z^{-1} Y^{-1} X Y \triangleright e.
\end{aligned}$$

Obviously $F(m)$ is also a vector space isomorphism. To prove that the maps associated to the other cases of Reidemeister-III move are well defined we can proceed similarly. It is possible to prove that all maps associated to Reidemeister-III move are well defined from remark 12, as it is the case for the other Reidemeister moves.

3.3 Morse Moves

Similarly with Reidemeister moves, if D and D' are knot diagrams related by a Morse move m , then there is naturally associated a map $\mathcal{V}(D) \xrightarrow{F(m)} \mathcal{V}(D')$.

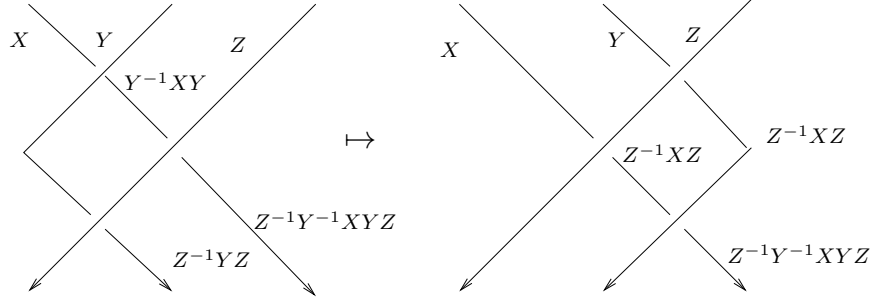


Figure 30: Map assigned to Reidemeister-III

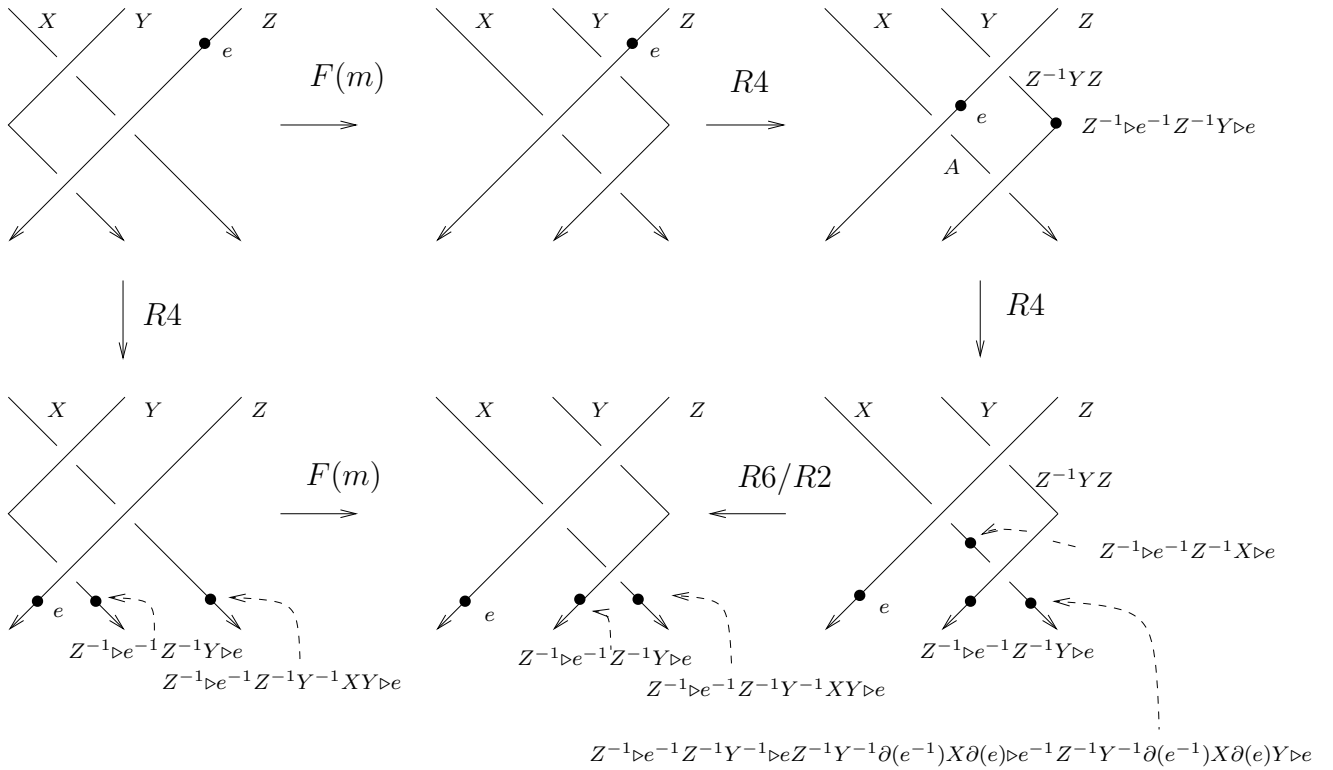


Figure 31: Proof that $F(m)$ is well defined if m is a Reidemeister-III move.
Here $A = Z^{-1}\partial(e^{-1})X\partial(e)Z$



Figure 32: Oriented saddle point Move

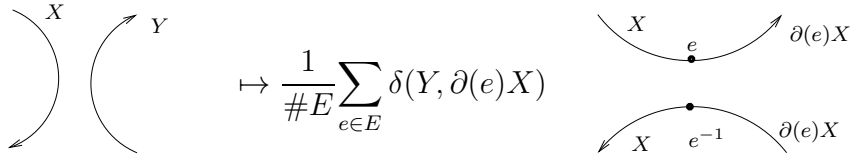


Figure 33: Map associated to saddle point moves

3.3.1 Saddle Points

There are two kinds of saddle points moves in the oriented case. They are depicted in figure 32. Let D and D' differ by a saddle point move. We can define a map $\mathcal{V}(D) \rightarrow \mathcal{V}(D')$. We make the definition for the first move, since it is analogous for the second one. It appears in figure 33. The map is well defined due to the identity in figure 34. This identity is proved in figure 35.

3.3.2 Cups and Caps

Since we are considering oriented diagrams, there are two kinds of births/deaths of a circle. They are described in figures 36 and 37. The maps assigned to births and deaths of circles are described in figures 39 and 38. There, 1 simply means what is left of the diagram. The other orientations are similar. It is easy to conclude that both types of maps are well defined.

$$\sum_{e \in E} \delta(Y, \partial(e)\partial(f)X) = \sum_{e \in E} \delta(Y, \partial(e)X)$$

Figure 34: An identity

3.4 Invariance

If we are given a movie of a knotted surface Σ , we can use the maps defined in the previous section to give an element $I(\Sigma)$ of the ground field κ . We assign the obvious map $\mathcal{V}(D) \rightarrow \mathcal{V}(D')$ if the knot diagram D' is related to D by a planar isotopy. To prove that it is an invariant of knotted surfaces, we need to prove invariance under the Movie Moves of Carter and Saito and interchanging distant critical points. The invariance under interchanging distant critical points is trivial to verify since all the maps defined are of a local nature. In the remainder of this subsection, we prove invariance under the Movie Moves. We use the numbering of the movie moves that appears in [BN]. Notice that since we consider oriented surfaces, we will need to consider not only the mirror image of the all the movie moves but also all the possible orientations of the strands.

3.4.1 Movie Moves 1 to 5

The invariance under these movie moves is a consequence of the definition of $F(m)$ for a Reidemeister move, since by definition $F(m^{-1}) = F(m)^{-1}$. Notice that we can always suppose that no vertices get in the way, by moving them away from the area in question and applying the commutation relations of 3.2.3.

3.4.2 Movie Moves 6 to 10

We can always suppose that no vertices get in the way. The proof of invariance is a straightforward calculation. The invariance under these movie moves is known already from the fact that, not considering saddle points, we are simply calculating the number of morphisms of the complement of a regular neighbourhood of the knotted surface Σ to G .

3.4.3 Going Right Movie Move 11

The movie move 11 appears in figure 40. We need to consider all the possible orientations. This movie move is reversible, so we consider the going right and going left cases. The proof of invariance under the going right case appears in figure 41. We only consider one orientation, but the other case is perfectly analogous.

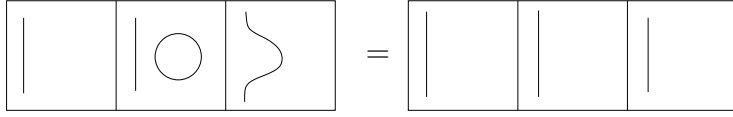


Figure 40: Movie Move 11

$$\begin{array}{c} \downarrow \end{array} \begin{array}{c} X \\ \mapsto \sum_{Y \in G} \end{array} \begin{array}{c} \downarrow \end{array} \begin{array}{c} X \\ \circlearrowright Y \end{array} \mapsto \frac{1}{\#E} \sum_{e \in E} \begin{array}{c} \downarrow \end{array} \begin{array}{c} X \\ \bullet \\ e \\ \bullet \\ e^{-1} \end{array} = \begin{array}{c} \downarrow \end{array} \begin{array}{c} X \end{array}$$

Figure 41: Invariance under Going Right Movie Move 11

3.4.4 Going Left Movie Move 11

The proof of invariance appears in figure 42.

3.4.5 Movie Move 12

The movie move 12 appears in figure 43. We need to consider its mirror image as well as a change on the orientation. The going right move is trivial to verify since there are no vertices involved. The invariance under going right movie move 12 is a bit more complicated since some vertices can get in the way. However, we can obviously suppose we have one only vertex, from relations $R1$ to $R6$; and the proof of invariance for this case appears in figure 44. The arguments used to prove invariance under the mirror images and the different orientations of this movie move are perfectly analogous.

$$\begin{array}{c} \downarrow \end{array} \begin{array}{c} X \\ \curvearrowright \end{array} = \frac{1}{\#E} \sum_{e \in \text{Ker}(\partial)} \begin{array}{c} \downarrow \end{array} \begin{array}{c} X \\ \bullet \\ e \\ \bullet \\ e^{-1} \end{array} \mapsto \begin{array}{c} \downarrow \end{array} \begin{array}{c} X \\ \bullet \\ 1_E \end{array} = \begin{array}{c} \downarrow \end{array} \begin{array}{c} X \end{array}$$

Figure 42: Invariance under Going Left Movie Move 11

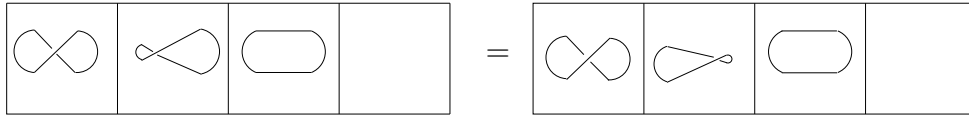


Figure 43: Movie Move 12

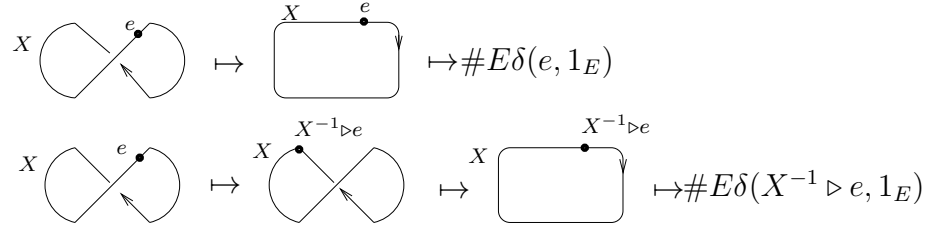


Figure 44: Proof of invariance under Going Right Movie Move 12.

3.4.6 Movie Move 13

The movie move 13 is presented in figure 45. It should be considered in both directions and considering also mirror images and opposite, though compatible, orientations. To begin with, we draw attention to the identity of figure 46. The proof of invariance under Going Right Movie Move 13 is a corollary of this identity, and appears in figure 47.

The invariance under Going Left Movie Move 13 appears in figure 48.

3.4.7 Movie Move 14

A version of the Movie Move 14 appears in figure 49. This is a reversible movie, so we need to treat the Going Right and Going Left cases separately. As usual, we need to consider all the possible changes in the orientations of the edges as well as on the crossing information.

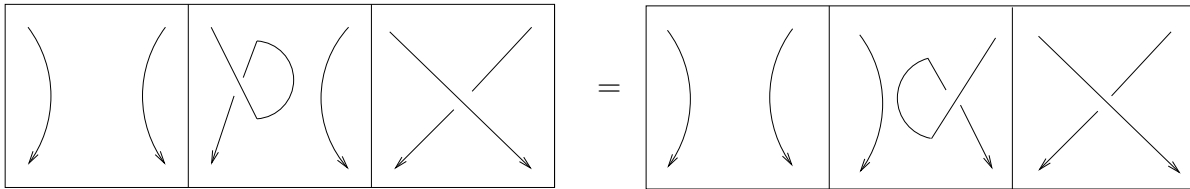


Figure 45: Movie Move 13

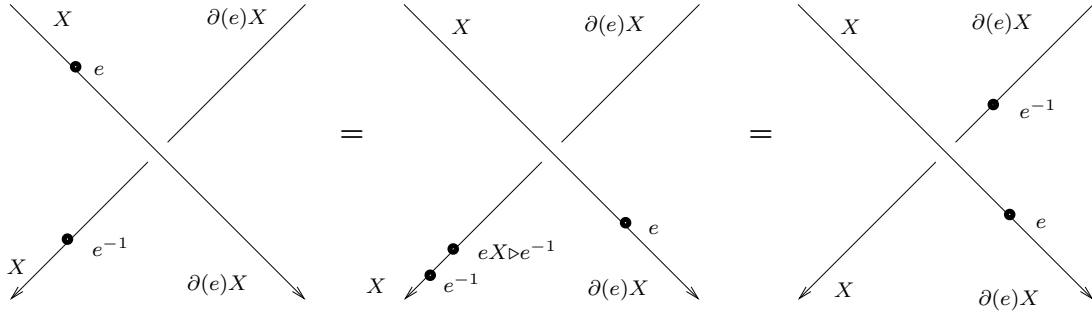


Figure 46: An identity

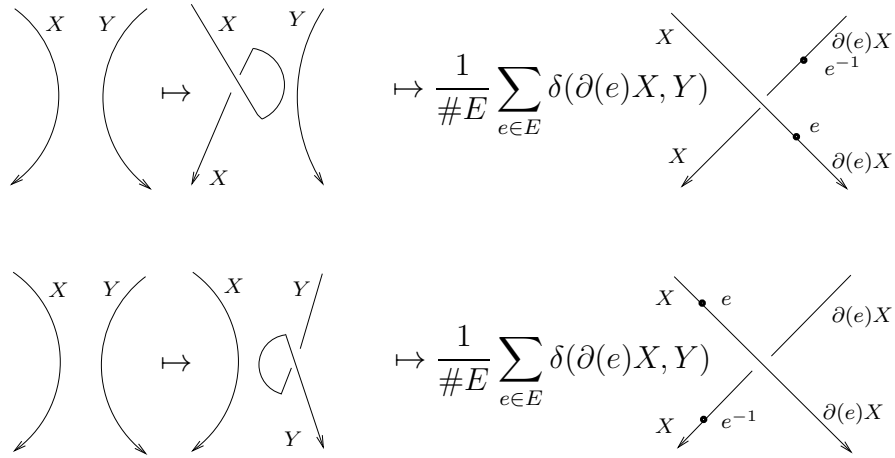


Figure 47: Invariance under Going Right Movie Move 13

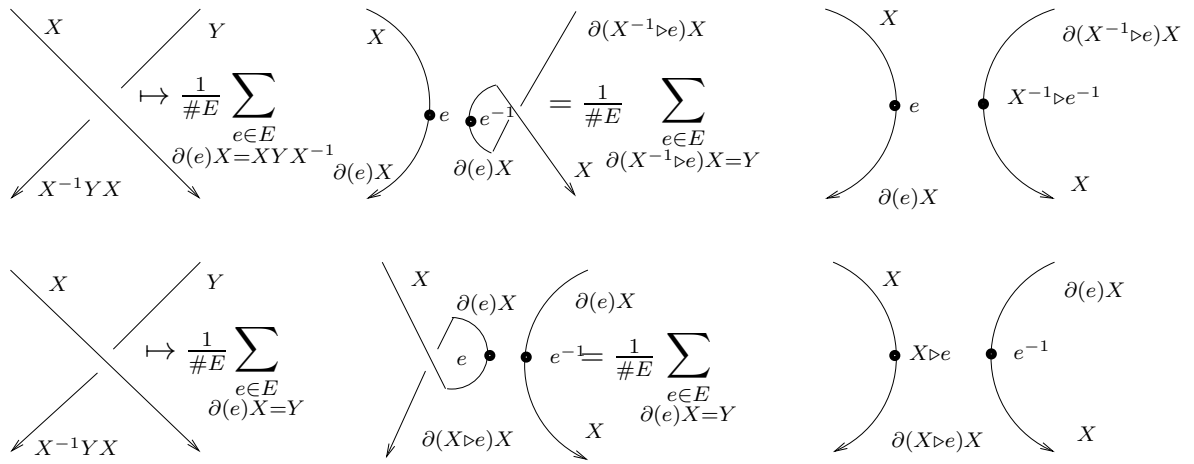


Figure 48: Invariance under Going Left Movie Move 13

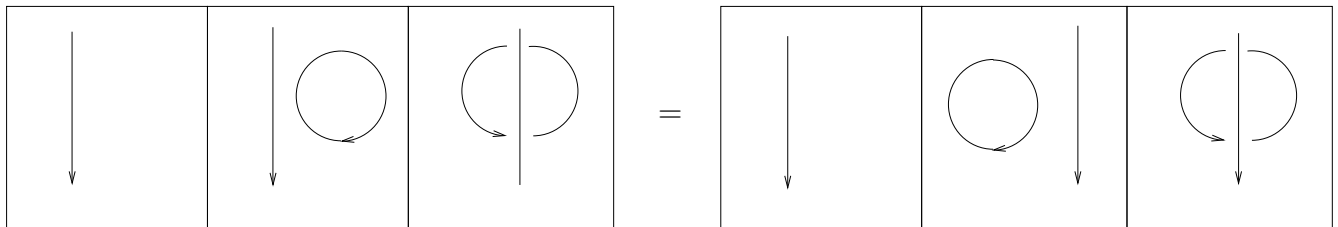


Figure 49: A version of Movie Move 14

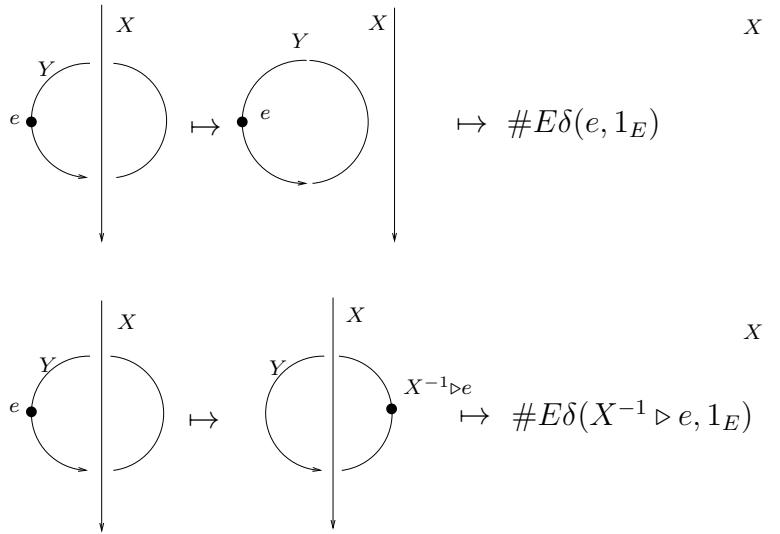


Figure 50: Invariance under Going Left Movie Move 14, first case

The going right case is the simplest, since we can suppose that no vertices get in the way. We leave the proof to the reader (c.f. section 3.4.2).

For the going left case, we can suppose that we initially have a unique vertex in the circle. The invariance under the two different types of Going Left Movie Move 14 appears in figures 50 and 51. The cases with different orientations are analogous.

3.4.8 Movie Move 15

A version of the oriented Movie Move 15 appears in figure 52. There are several other versions obtained by reversing the orientations of the strands and considering mirror images. We say a movie move 15 is of the first kind if it is obtained from figure 52 by (possibly) changing the orientation of the strands, and it is of the second kind if, similarly, it is obtained from the mirror image of figure 52.

Let us consider the going right case first. If the movie move is of the first kind, the invariance is a consequence of the identity in figure 53, and the calculation appears in figure 54. The proof of invariance under the other kinds of going right Movie Move 15 appears in figure 55.

Analogously, the invariance under the first kind of Going Left Movie Move 15 is a consequence of the identity of figure 56. The invariance under the

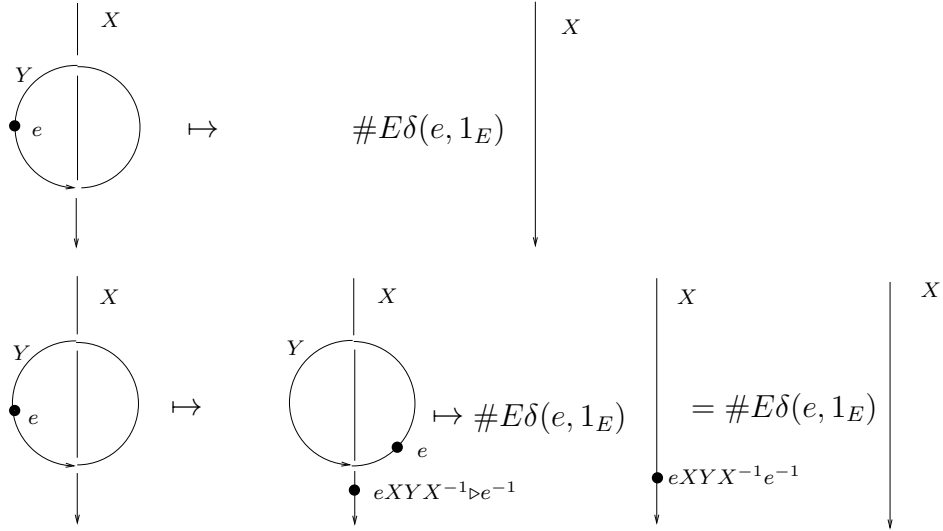


Figure 51: Invariance under Going Left Movie Move 14, second case

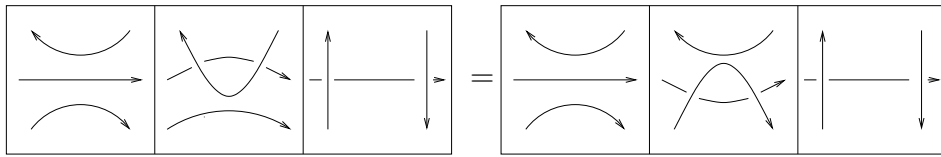


Figure 52: A version of Movie Move 15

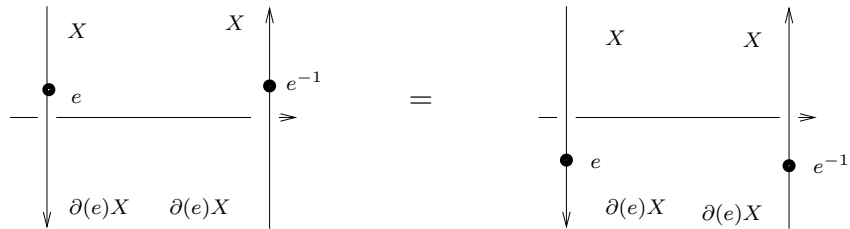


Figure 53: An identity

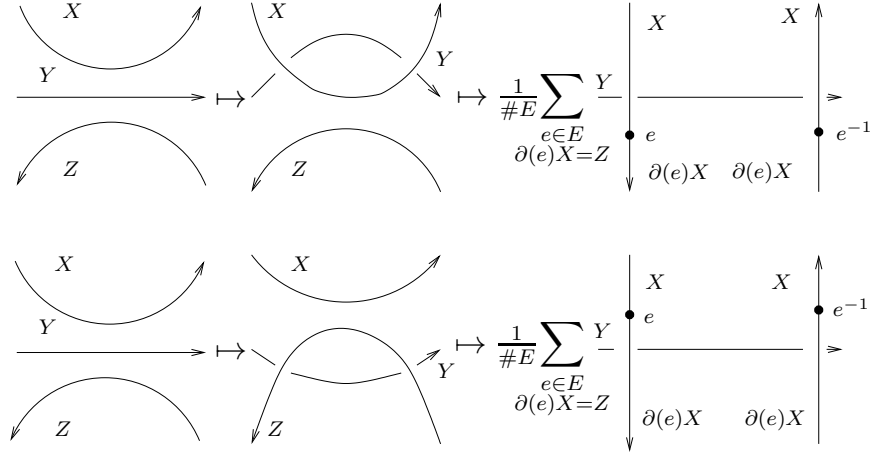


Figure 54: Invariance under Going Right Movie Move 15, first case

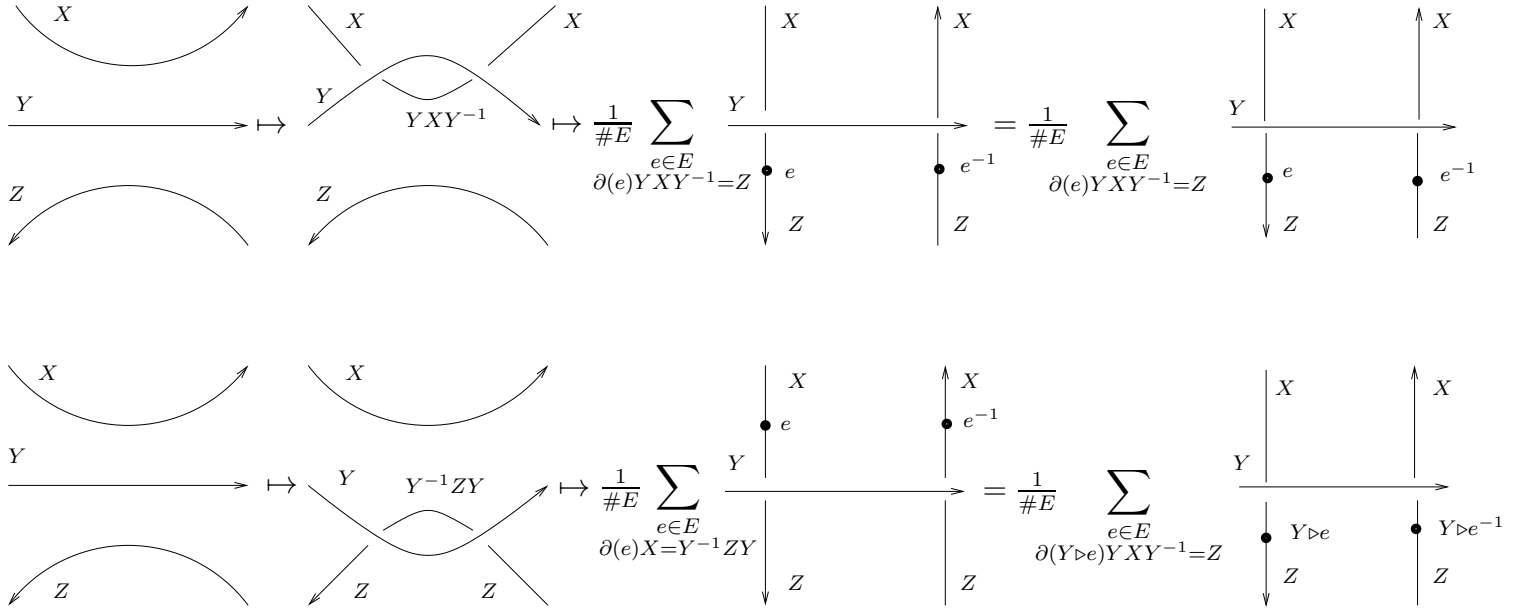


Figure 55: Invariance under Going Right Movie Move 15, second case

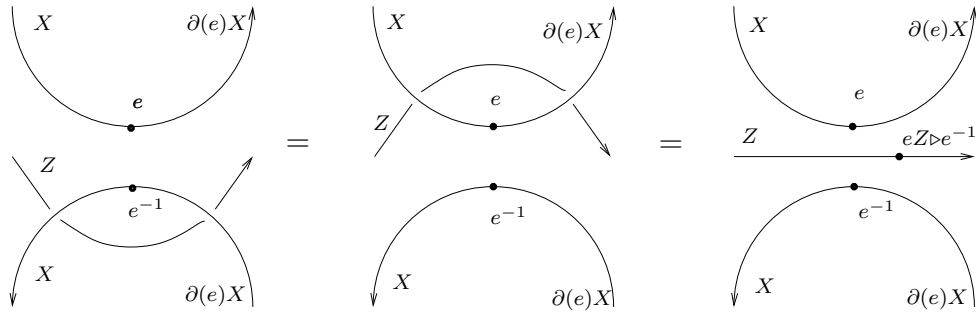


Figure 56: An identity

second kind of Going Left Movie Move 15 appears in figure 57. The cases with different orientation are dealt with similarly. This will finish the proof that $I(\Sigma)$ is an isotopy invariant of knotted surfaces.

Theorem 14 *Let $\mathcal{G} = (G, E, \partial, \triangleright)$ be a finite crossed module. Let Σ be an oriented knotted surface. The evaluation $I(\Sigma)$ does not depend on the movie presentation of Σ , and therefore I is an isotopy invariant of oriented knotted surfaces.*

Acknowledgements

This work was done at the Mathematics Department of Instituto Superior Técnico (Lisbon), with the financial support of FCT (Portugal), post-doc grant number SFRH/BPD/17552/2004. It is part of the research project POCTI/MAT/60352/2004 ("Quantum Topology"), also financed by FCT.

I would like to express my gratitude to Dr Roger Francis Picken and Dr Marco Mackaay for many helpful discussions and their constant (and very encouraging) support from much before this work had even started. I would like to thank Dr Scott Carter for having been extremely helpful by answering numerous questions that appeared whilst I was preparing this article, and for having commented on a preliminary version of it.

This article has an indirect, although strong, influence of Dr John W. Barrett, namely in the philosophy of working with handle decompositions instead of triangulations, a lesson, amongst many others, that I received from him whilst being his PhD student.

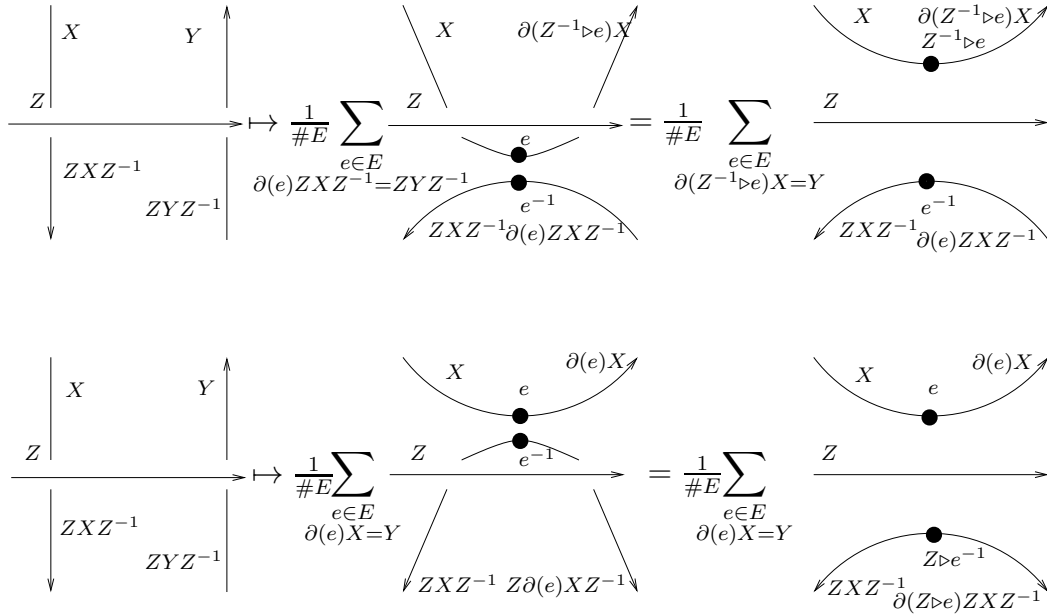


Figure 57: Invariance under the second kind of Going Left Movie Move 15

References

- [BN] Dror Bar-Natan: Khovanov Homology for Tangles and Cobordisms, math.GT/0410495 v1.
- [BGM] John W. Barrett, J. Manuel Garcia-Islas, João Faria Martins: Observables in the Turaev-Viro and Crane-Yetter models, math.QA/0411281
- [BM] John W. Barrett, Marco Mackaay: Categorical Representations of Categorical Groups, math.CT/0407463.
- [BS] Ronald Brown; Christopher B. Spencer: G -groupoids, crossed modules and the fundamental groupoid of a topological group. Nederl. Akad. Wetensch. Proc. Ser. A 79=Indag. Math. 38 (1976), no. 4, 296–302.
- [BW1] John W. Barrett, Bruce Westbury: Spherical Categories, Adv. Math. 143 (1999), no. 2, 357–375.

- [BW2] John W. Barrett, Bruce Westbury: Invariants of piecewise-linear 3-manifolds. *Trans. Amer. Math. Soc.* 348 (1996), no. 10, 3997–4022.
- [CS] J. Scott Carter, Masahico Saito: *Knotted Surfaces and their Diagrams*, *Mathematical Surveys and Monographs*, 55. American Mathematical Society, Providence, RI, 1998.
- [FY] Peter Freyd, David Yetter: Coherence theorems via knot theory. *J. Pure Appl. Algebra* 78 (1992), no. 1, 49–76.
- [GS] Robert E. Gompf, András I. Stipsicz: *4-Manifolds and Kirby Calculus*, *Graduate Studies in Mathematics*, 20. American Mathematical Society, Providence, RI, 1999.
- [P] Tim Porter: Interpretations of Yetter’s notion of G -coloring: simplicial fibre bundles and non-abelian cohomology. *J. Knot Theory Ramifications* 5 (1996), no. 5, 687–720.
- [Y] David Yetter: TQFT’s from Homotopy 2-types, *J. Knot Theory Ramifications* 2 (1993), no. 1, 113–123.